# Robust Design Optimisation of Gas Turbine Compression Systems

Tiziano Ghisu,* Geoffrey T. Parks,† Jerome P. Jarrett,‡ P. John Clarkson§

*Engineering Design Centre, Cambridge University Engineering Department*

*Trumpington Street, Cambridge CB2 1PZ, UK*

**Engineering design commonly assumes nominal values for uncertain parameters to simplify the design process: the design of a gas turbine, or one of its modules, is generally approached with some specific operating conditions in mind (its design point). Unfortunately, engine components never exactly meet their specifications and do not operate at just one condition, but over a range of power settings. This simplification can then lead to a product that exhibits performance significantly worse than nominal in real-world conditions. This problem is exacerbated in the presence of heavily optimised designs, which tend to lie in extreme regions of the design space.[14] In gas turbine design, safe and satisfactory off-design operation must be guaranteed and is generally evaluated before moving to the next phase of the design process. This approach, while guaranteeing that some minimum requirements are met, introduces a further loop in the design process and does not ensure the final design will be optimal with respect to this new requirement. The introduction of some robustness considerations into the design process can reduce the level of fragmentation and iteration typical of gas turbine engine design and produce further (and more robust) improvements relative to the traditional method. In this study, two approaches for dealing with off-design performance analysis are presented, integrated into an automatic optimisation system and applied to the preliminary design of a core compression system from a three-spool modern turbofan engine. Designs that are more robust than those found if only design-point performance is considered are successfully identified.**

## Nomenclature

*Roman*

| | |
|---|---|
| $\bar{m}$ | (pseudo) non-dimensional mass-flow |
| $\dot{m}$ | mass-flow |
| $\mathbf{x}$ | design vector |
| $c_p$ | specific heat capacity at constant pressure |
| $DF$ | Diffusion Factor |
| $DH$ | De Haller number |
| $f$ | objective function |
| $H$ | boundary layer shape factor |
| $H_n$ | Hermite polynomial |
| $H_v$ | fuel lower calorific value |
| $I_n$ | generic Wiener-Askey polynomial |
| $k$ | generic input variable |
| $Koch$ | Koch factor |
| $m$ | number of modules |
| $MSD$ | mean square deviation |

*PhD research student, Cambridge University Engineering Department, Trumpington Street, Cambridge CB2 1PZ, UK

†Senior Lecturer, Cambridge University Engineering Department, Trumpington Street, Cambridge CB2 1PZ, UK

‡Lecturer, Cambridge University Engineering Department, Trumpington Street, Cambridge CB2 1PZ, UK

§Professor, Cambridge University Engineering Department, Trumpington Street, Cambridge CB2 1PZ, UK

| | |
|---|---|
| $N$ | number of random dimensions |
| $n$ | total number of stages |
| $N_0$ | quadrature order |
| $P$ | total pressure |
| $p$ | probability density function |
| $P_i$ | orthogonal polynomial |
| $PR$ | Pressure Ratio |
| $SM$ | Surge Margin |
| $SPR$ | static pressure rise coefficient |
| $T$ | temperature |
| $W$ | weighting function |
| $X$ | a random process |

*Greek*

| | |
|---|---|
| $\eta$ | isentropic efficiency |
| $\eta_{is,tot}$ | total system isentropic efficiency |
| $\gamma$ | ratio of specific heats |
| $\mu$ | mean value |
| $\Phi$ | Wiener-Askey Chaos |
| $\Psi$ | Hermite Chaos |
| $\sigma^2$ | variance |
| $\theta$ | a generic random event |
| $\xi$ | random variable |
| $\boldsymbol{\xi}$ | vector of noise factors |

*Subscripts*

| | |
|---|---|
| 0 | total (stagnation) conditions |
| c | cold gas (referred to $c_p$) |
| comb | combustion |
| dp | design point |
| h | hot gas (referred to $c_p$) |
| is | isentropic |
| pl | part-load |

*Acronyms*

| | |
|---|---|
| CFD | Computational Fluid Dynamics |
| FOFM | First Order First Moment |
| FOSM | First Order Second Moment |
| H&J | Hooke and Jeeves |
| HC | Hermite Chaos |
| HPC | high pressure compressor |
| IPC | intermediate pressure compressor |
| LTM | Long Term Memory (Tabu Search algorithm) |
| MCS | Monte Carlo Simulations |
| MTM | Medium Term Memory (Tabu Search algorithm) |
| NIPC | Non-intrusive Polynomial Chaos |
| PC | Polynomial Chaos |
| PDF | probability density function |
| SOFM | Second Order First Moment |
| SOSM | Second Order Second Moment |
| STM | Short Term Memory (Tabu Search algorithm) |
| TS | Tabu Search |

# I. Introduction

The design of a new gas turbine is a challenging task described in more detail in a companion paper.[9] Engineering design commonly assumes nominal values for uncertain parameters to simplify the design process.

Unfortunately, this simplification can lead to a product that exhibits performance significantly worse than nominal in real-world conditions. This problem is exacerbated in the presence of heavily optimised designs, which tend to lie in extreme regions of the design space.[14] In real-world applications, it is important not only to achieve good performance, but also to be able to maintain it over a range of operating conditions and during the whole course of the life of the product. Some consideration of the impact of off-design conditions on performance should therefore be embedded in the design process to avoid bigger problems during the later development or testing phases. Two different (but equivalent) illustrations of the concept of robust design are given in Figure 1.

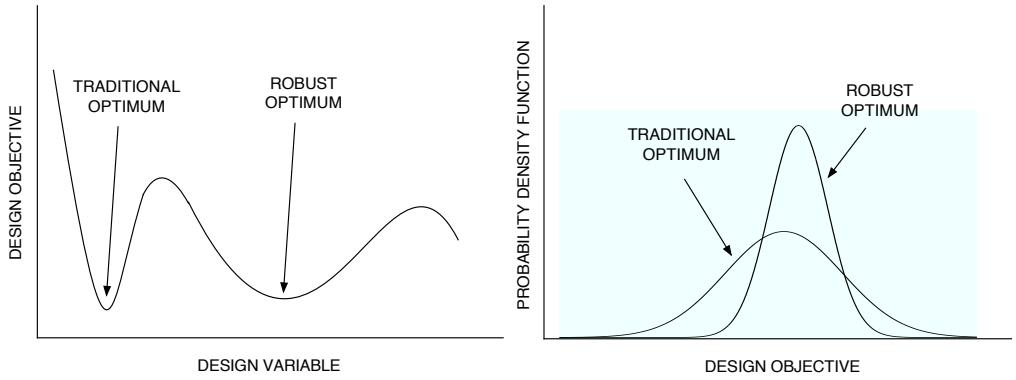


Figure 1: Two different (but equivalent) illustrations of the concept of robust design

The starting point for the development of robust design methodologies is the work of Dr Genichi Taguchi, a Japanese engineer who, between the 1950s and 1960s, built the theoretical foundations of Robust Design and applied them successfully in the design of a number of products. Ross[24] and Phadke[22] give a good overview of the Taguchi method and of its implications. Phadke defines Robust Design as a method for improving the quality of a product through the minimisation of the effect of the causes of performance variability without eliminating the causes themselves.

The causes of performance variability are usually defined as *noise factors*. A robust design is a design that is less sensitive to the presence of noise factors, which are categorised by Phadke[22] into three groups:

- *External*: External sources of performance variation, independent of the product itself.
- *Unit-to-unit variation*: Variation due to manufacturing variability (or manufacturing tolerances).
- *Deterioration*: Variation due to the change in product performance with time and wear.

In Taguchi's work there is no reference to the reliability of the method (or model) used to quantify this quality. Modern engineering relies heavily on a number of ever more sophisticated computational models. These can represent an additional source of uncertainty in the product's performance. A more realistic classification of uncertainty sources is given by Oberkampf and Trucano,[21] who distinguish between *aleatory* and *epistemic* uncertainty: the former is associated with the physical system under consideration and its operating environment (already identified by Phadke), while the latter arises from lack of knowledge in the modeling process and can be made negligible if sufficient data are available.[14] Walters and Huyse[26] concentrate on the role of uncertainty in CFD, further subdividing epistemic uncertainty into discretisation and model uncertainty: discretisation errors can be driven to zero (or to very low levels) with sufficient computational resources, while model uncertainty can be only estimated by comparing experimental and computational results.

Robust design can be considered as the methodology for finding the set of control factors (or design variables) that minimise the sensitivity of the product to the noise factors. Putko *et al.*[23] subdivide the whole process into 3 steps:

- *Uncertainty quantification*: Determination of noise factors and their distribution.
- *Uncertainty propagation*: Determination of the effect of the noise factors on the performance of the product.

- *Robust optimisation* itself: Identification and selection of the "best solution".

The importance of Taguchi's work lies in the consideration of quality as a characteristic to be included directly in the design of a product: in his approach this was ensured through the minimisation of a signal-to-noise ratio, defined as $-10log_{10}MSD(\mathbf{x},\boldsymbol{\xi})$, where $MSD(\mathbf{x},\boldsymbol{\xi})$ is the mean square deviation of the objective function $f(\mathbf{x},\boldsymbol{\xi})$ from a target value $f_{target}$ (see equation (1)), $\mathbf{x}$ the vector of control variables and $\boldsymbol{\xi}$ the vector of noise factors. Taguchi used Orthogonal Arrays as a method for reducing the number of experiments necessary to evaluate the quality metric; Phadke[22] suggests the use of Monte Carlo Simulations (MCS) and Taylor Series Expansions as alternatives to Orthogonal Arrays. Standard Analysis of Variance (AnoVa) techniques are then used to derive the signal-to-noise ratio.[14]

$$MSD(\mathbf{x},\boldsymbol{\xi}) = \langle (f(\mathbf{x},\boldsymbol{\xi}) - f_{target})^2 \rangle = lim_{m\to\infty} \frac{\sum_{i=1}^{m} (f(\mathbf{x},\boldsymbol{\xi}^{(i)}) - f_{target})^2}{m} \tag{1}$$

An alternative approach is to consider the problem as a multi-objective optimisation problem, aiming to minimise simultaneously the mean $\mu_f$ and variance $\sigma_f^2$ of the objective function. Design for six sigma (an approach widely adopted in industry) aims to maintain six standard deviations of $f$ within acceptable limits (or equivalently to minimise the weighted objective function $\mu_f + 6\sigma_f$).[30]

Walters and Huyse[26] give an exhaustive overview of the principal methods available for uncertainty analysis (focusing on fluid mechanics applications), separating deterministic methods (such as interval analysis and sensitivity derivatives), which are based on a number of deterministic evaluations and are relatively inexpensive, from probabilistic ones (MCS, moments methods and Polynomial Chaos), which attempt to approximate the probability distribution of the objective function, but are computationally more expensive and require a more detailed estimation of the probability distribution of the noise factors.

The basic idea of the *interval analysis* approach is to evaluate the performance of the system for a number of combinations of the noise factors to produce an estimation of the maximal error bounds for the nominal performance (or, equivalently, a worst case scenario evaluation). A similar estimation can be performed with *sensitivity derivatives* and a first order Taylor series approximation of the objective function

$$\Delta f = \sqrt{\sum_{i=1}^{N} \frac{\partial f}{\partial \xi_i} \Delta \xi_i} \tag{2}$$

where $N$ is the number of uncertain parameters and the $\Delta\xi_i$ their uncertainty bounds.

Given an accurate estimation of the noise factors' probability distributions, *Monte Carlo Simulations* represent the only method that allows an exact estimation of the probability distribution of the objective function (and then of its moments). The major limitation is the number of simulations needed to achieve an accurate estimation (the convergence rate of MCS is $O(1/\sqrt{m})$, which means that the number of samples has to be increased by a factor of 100 to improve the accuracy by one decimal place[14]): this is why for real-world applications this technique is always used in association with some sort of response surface.

*Moment methods* are based on an approximation of the objective function $f$ through a Taylor series expansion about its nominal value $\bar{f} = f(\bar{\xi})$. If only one uncertain parameter is considered, first and second order expansions of the objective function are respectively

$$f(\xi) = f(\bar{\xi}) + \frac{\partial f}{\partial \xi}(\Delta\xi) + O(\Delta\xi^2) \tag{3}$$

$$f(\xi) = f(\bar{\xi}) + \frac{\partial f}{\partial \xi}(\Delta\xi) + \frac{1}{2}\frac{\partial^2 f}{\partial \xi^2}(\Delta\xi)^2 + O(\Delta\xi^3) \tag{4}$$

First Order First Moment (FOFM), First Order Second Moment (FOSM), Second Order First Moment (SOFM) and Second Order Second Moment (SOSM) approaches take their names from the order of the expansion considered and of the moment analysed. SOFM and SOSM can be calculated as follows

$$\mu_f = \int_{-\infty}^{\infty} f(\xi)p(\xi)d\xi = \int_{-\infty}^{\infty} [f(\bar{\xi}) + \frac{\partial f}{\partial \xi}(\Delta\xi) + \frac{1}{2}\frac{\partial^2 f}{\partial \xi^2}(\Delta\xi)^2]p(\xi)d\xi = f(\bar{\xi}) + \frac{\sigma^2(\xi)}{2}\left.\frac{\partial^2 f}{\partial \xi^2}\right|_{\bar{\xi}} \tag{5}$$

$$\sigma_f^2 = \int_{-\infty}^{\infty} [f(\xi) - f(\bar{\xi})]^2 p(\xi) d\xi \quad = \quad \int_{-\infty}^{\infty} [\frac{\partial f}{\partial \xi}(\Delta\xi) + \frac{1}{2}\frac{\partial^2 f}{\partial \xi^2}(\Delta\xi)^2]^2 p(\xi) d\xi = \left( \frac{\partial f}{\partial \xi}\bigg|_{\bar{\xi}} \right)^2 \sigma^2(\xi) \qquad (6)$$

where $p(\xi)$ represents the noise factor's probability density function (PDF).

Clearly the above approximations are exact only when the noise factors are Gaussian-distributed and the objective function is well represented by a second order Taylor series. The more the noise factors and the objective function(s) depart from these assumptions, the less reliable these estimates are.

In recent years, Polynomial Chaos (PC) has received much attention as it offers an exact means of propagating uncertainties through a system, providing high order information (similar to MCS) at a much reduced cost.[29] The basic idea is to express the stochastic variable(s) as an expansion in terms of orthogonal polynomials: the first formulation by Wiener[27] employed Hermite polynomials in terms of standard Gaussian variables and proved very efficient in the propagation of Gaussian-distributed uncertainties; an extension has been formulated by Xiu[28] to analyse a wider spectrum of input distributions. The resulting equations are simplified via a Galerkin projection on the elements of the orthogonal basis and the main moments evaluated based on the resulting PC expansion.[6] A non-intrusive alternative has also been developed, based on the observation that the coefficients of the different modes can be obtained by projecting deterministic computations onto the PC basis,[16] and offers considerable advantages in the presence of complex systems or non-easily accessible evaluation tools.

## II. Model

This study concentrates on the robust preliminary aerodynamic optimisation of the core compression system of a three-spool modern aeroengine, shown in Figure 2 and composed of an intermediate pressure compressor (IPC), an s-shaped duct and a high pressure compressor (HPC). The advantages of an integrated design (and optimisation) approach have been demonstrated by Jarrett *et al.*[13] and Ghisu *et al.*:[9] the elimination of the "artificial contraints" dictated by the structure of the design process rather than by real physical limits allows the full exploitation of the capabilities of the system, while the use of sophisticated search algorithms (design optimisation) can provide a faster means of conducting a more thorough exploration of the design space, with significant benefits for both achievable performance and design times. Only the main characteristics of the system are summarised here; a detailed description is provided in.[9]

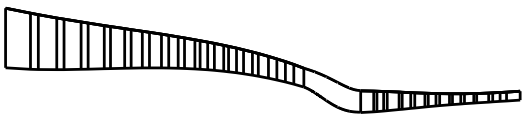

Figure 2: Meridional view of a core compression system (IPC, duct and HPC)

- *Evaluation Tool*: A proprietary code for mean-line performance prediction is used to evaluate the compressor preliminary design. Given geometry and operating point, the code estimates the performance in terms of efficiency and operating margin, both at design-point and off-design conditions. A prediction for the surge margin is made based on a number of different correlations. The duct is modeled using the Finite Volume axi-symmetric CFD solver developed by Ghisu *et al.*[8] in combination with a Reduced Order Model based on the Radial Basis Function approach to minimise the number of CFD calls. The absence of (or a sufficient margin from) separated flow in the duct is ensured by limiting the value of the maximum shape factor $H$ for the duct boundary layers.

- *Geometry Modeler*: The shape of each compressor annulus is specified through the definition of mean-line and area distributions: a fourth order polynomial is used in the mean-line definition, while a fifth order one is used to define the area distribution, in order to give greater flexibility in each stage flow

function. As required by the analysis software, pressure ratios across each stage and stator exit angles are specified. For each blade row, the number of blades and axial chords are allowed to vary. Solidities and aspect ratios can easily be calculated as a function of axial chord and blade stagger and number. Thickness-on-chord ratios and tip clearances were kept fixed, as they involve structural, material and manufacturing considerations that go beyond the scope of this work. The same parameterisation used for the compressor annulus is also used for the duct endwalls, with $C^1$ continuity being imposed at the interfaces to ensure smooth hub and casing surfaces. The design space is summarised in Table 1.

Table 1: Design space definition ($m$ represents the number of modules and $n$ the total number of stages)

| Variable Type | Count |
|---|---|
| mean-line | $2m+2$ |
| area distribution | $3m+2$ |
| stage pressure ratios | $n$ |
| stator flow exit angles | $n$ |
| blade axial chords | $2n$ |
| blade numbers | $2n$ |
| Total | $5m+6n+4$ |

Some of the total $5m+6n+4$ variables were then fixed to meet the requirements of the contiguous components, depending on the specific optimisation problem (inlet and exit values for radius and inlet and exit swirl angles are typical examples), while lower and upper bounds were set to avoid the search of clearly infeasible regions.

- *Optimiser*: The TS algorithm developed by Jaeggi[12] was selected for this work. TS is a meta-heuristic method designed to help a search negotiate difficult regions by imposing restrictions.[10] The local search phase at its heart is conducted with the Hooke and Jeeves (H&J) algorithm:[11] a suitable increment is chosen for each variable and the value of the objective function is calculated in turn for $x_i^{'} = x_i + \delta_i$ and $x_i^{'} = x_i - \delta_i$ while keeping the other variables at their base values. The best allowed move is made. The *Short Term Memory* (STM) records the last $S$ visited points, which are tabu and thus cannot be revisited. The effect of the STM is that the algorithm behaves like a normal hill-descending algorithm until it reaches a minimum, then it is forced to climb out of the hollow and explore further. Two other important characteristics of the TS algorithm are *intensification* and *diversification*. *Intensification* is associated with the *Medium Term Memory* (MTM) where the best $M$ solutions located are stored. *Diversification* is associated with the *Long Term Memory* (LTM), which records the areas of the search space that have been searched reasonably thoroughly by dividing the design space into a number of sectors and recording how many times each sector has been visited. On diversification the search is restarted in an under-explored region of the design space. The extension to multi-objective problems is straightforward: the MTM contains the set of non-dominated solutions found, while at every H&J move, in the absence of a single non-dominated solution, a random move is selected among the set of non-dominated new designs. The discarded designs are not lost, as they are stored in the MTM, if appropriate, and can then be selected during intensification.

### II.A. Traditional Optimisation

The optimisation of the design-point performance of the system in Figure 2 was presented in.[9] The optimisation aimed to maximise system efficiency and IPC and HPC surge margin, subject to a number of aerodynamic constraints, limiting the load on the different blade rows and on the duct boundary layer (summarised in Table 2), for a total of 95 design variables and 3 objectives. Figure 3 reports the Pareto front found (the colour scale indicates the level of efficiency improvements): substantial increments in all the objectives can be achieved thanks both to the use of an intelligent search algorithm (which allows a more thorough exploration of the design space) and to the integrated design approach (which allows the elimination of the "artificial constraints", needed to simplify the design problem by subdividing it into smaller tasks – the design of each module – but detrimental from an optimisation point of view).

Figure 4 presents the solution of the same optimisation problem for a variable number of stages in the IPC (which initially had 8 stages, while the HPC had 6). The same results are also shown in Figure 5 in the

Table 2: Definition of the optimisation problem

| | |
|---|---|
| maximise | $\eta_{is,tot}$ |
| | $SM_{IPC}$ |
| | $SM_{HPC}$ |
| subject to | $DH_{min} \geq \overline{DH}$ |
| | $SPR_{max} \leq \overline{SPR}$ |
| | $DF_{max} \leq \overline{DF}$ |
| | $Koch_{max} \leq \overline{Koch}$ |
| | $H_{max_{DUCT}} \leq \overline{H}$ |

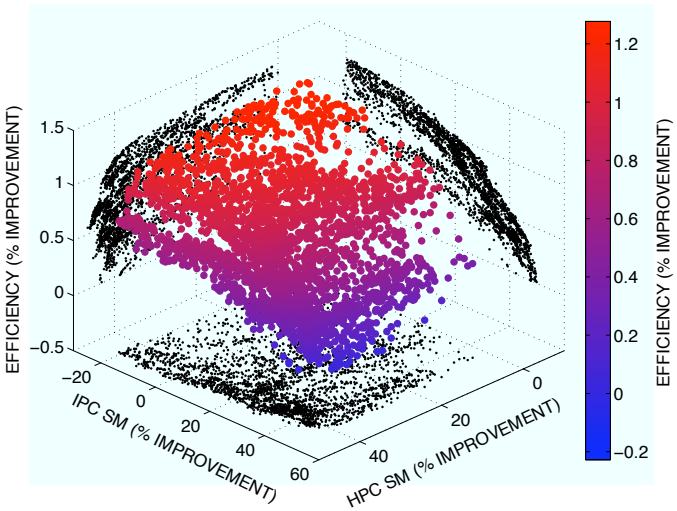


Figure 3: Results from the optimisation of the core compression system

form of contour plots: the maximum achievable efficiency for a combination of IPC and HPC surge margins is shown, for designs with different numbers of stages. It is evident how the larger compressor exit Mach number allows a reduction in the number of stages (from 8 to 7) with a minimal increase in losses. A further reduction in the number of stages requires a larger compromise in the achievable performance level (Figure 5(c)).

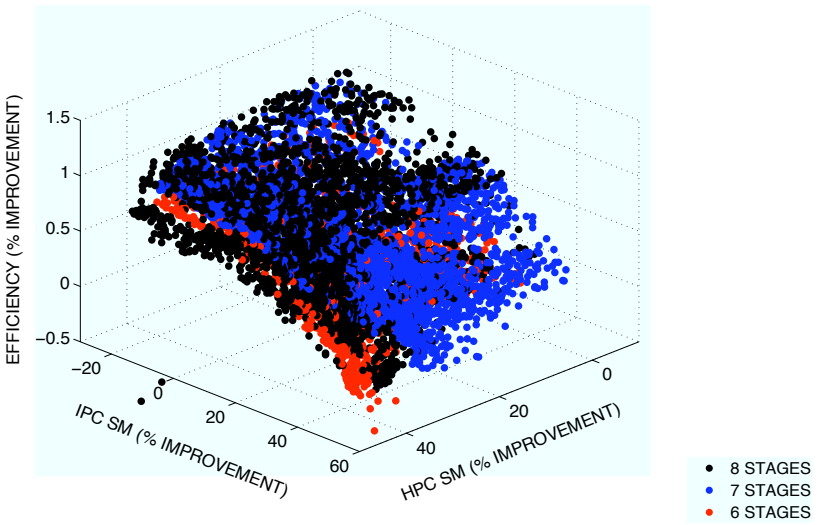


Figure 4: Reducing the number of IPC stages

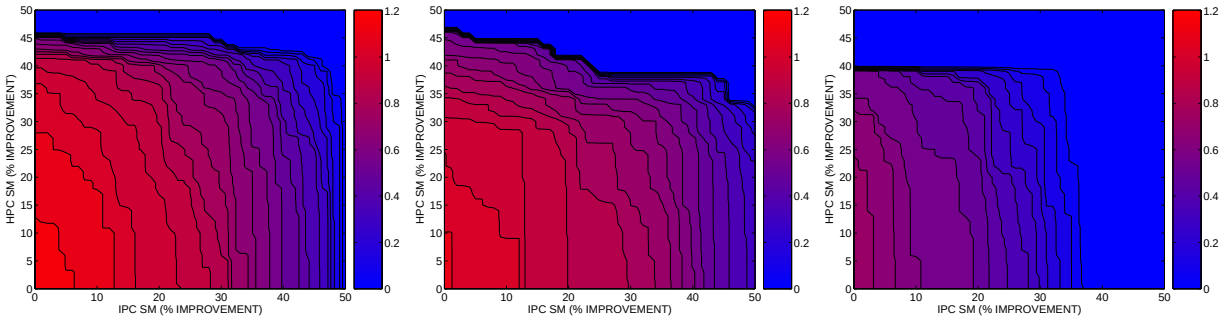


(a) 8 stages (b) 7 stages (c) 6 stages

Figure 5: Reducing the number of IPC stages (contour plots of system efficiency)

# III. Methodology

The design of a compression system (and of a gas turbine or an aircraft more generally) is usually approached with some specific operating conditions in mind (its design point): in the previous section, the core compression system from a three-spool modern turbofan engine was optimised with respect to its design-point performance. Unfortunately, engine components never exactly meet their aerodynamic design specifications and do not operate at just one condition, but over a range of power settings: satisfactory performance and safe operation must be guaranteed at all off-design conditions,[4] including engine starting, idling, reduced power, maximum power, acceleration and deceleration.[2] Compressor blades have a limited range of incidence before losses rise markedly, causing a rapid deterioration in compressor efficiency, if not unacceptable problems such as stall and surge. Even in the absence of such problems, is it guaranteed that optimising design-point performance does not worsen off-design performance? In this case, is the "optimised" design really better than the initial one? Is the optimisation of the design-point performance the real goal of the design process, or do we perhaps need to reformulate the problem?

The compressor being part of a larger system, it is important to understand how its operating conditions depend on the general engine operating point. This section first presents a review of compressor off-design operation, then two methods for dealing with off-design working conditions within the design process are introduced and integrated into the system.

## III.A. Uncertainty Quantification

As with other aerodynamic metrics, compressor performance is generally expressed in non-dimensional (or corrected) terms: the compressor map reports pressure ratio and efficiency as a function of the non-dimensional mass-flow for several values of the constant non-dimensional speed. More details on the derivation of these non-dimensional groups, the generation of compressor maps and the reasons for their specific form can be found in a number of specialised texts.[2–5, 19, 25]

Figure 6 shows the compressor map of a generic IPC. The most important features are: the constant corrected speed lines (extending from choke to surge), with the last almost parallel to the vertical axis because of the first stages' choking at high rotational speeds; the surge line, which represents the location of surge (or rotating stall at low rotational speeds) at different rotational speeds because of excessive flow separation due to the increased flow incidence on the blade at reduced mass-flows; and the working line, which represents the locus of stable (or non-transitional) compressor operation at the different rotational speeds. Excursions from working-line operation happen during acceleration/deceleration or because of power off-take or bleed.

### *III.A.1. Determination of the Working-line*

The working-line is the locus of stable operation of the compressor (which happens when compressor and turbine mounted on the same shaft have the same rotational speed, mass-flow and power produced/required). The determination of the working-line for any of the engine components (generally known as engine matching) is typically an iterative process (each component's operation is influenced mutually by other engine components). The operation of a compressor is greatly influenced by the turbine mounted on the same

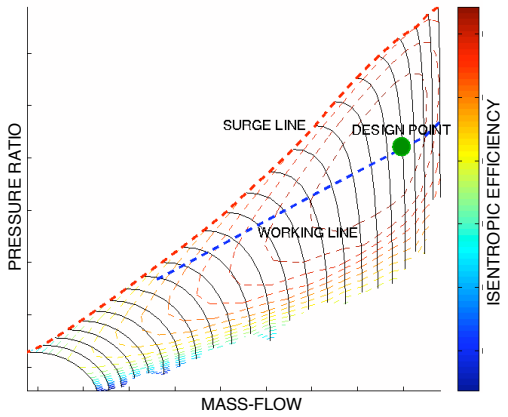


Figure 6: Typical IP compressor map: pressure ratio as a function of corrected mass-flow is shown for several constant corrected speed lines together with isentropic efficiency contours

shaft. Unfortunately, during compression system design it is quite common to have only limited information about the turbine. Two common assumptions are to have a turbine working between choked nozzles and with a constant efficiency. Clearly, if the turbine characteristics are known, all this information can be obtained through an iterative process that also involves compressor characteristics. If the change in combustion losses with fuel flow is significant, these need to be taken into account too.[4]

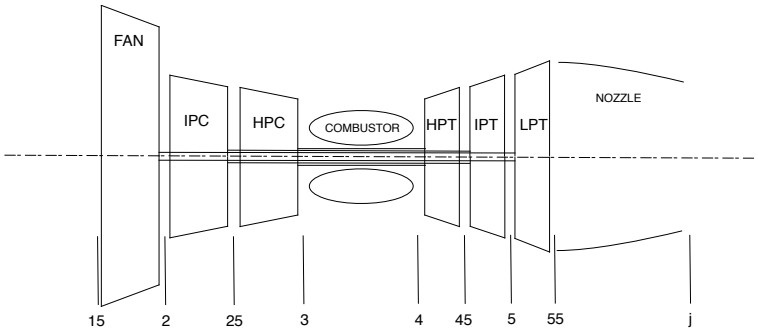


Figure 7: Schematic of a three-spool gas turbine

With these assumptions, the compressor working-line can be calculated. Detailed derivation is omitted.

$$\begin{cases} \frac{P_{0,25}}{P_{0,2}} = \left(1 + k_1 \frac{c_{p,h}}{c_{p,c}} \frac{T_{0,4}}{T_{0,2}} \eta_{LPC}\right)^{\frac{\gamma}{\gamma-1}} \\ \overline{m}_2 = k_2 \frac{P_{0,3}}{P_{0,2}} \sqrt{\frac{T_{0,2}}{T_{0,4}}} \\ \frac{P_{0,3}}{P_{0,25}} = \left(1 + k_3 \frac{c_{p,h}}{c_{p,c}} \frac{T_{0,4}}{T_{0,25}} \eta_{HPC}\right)^{\frac{\gamma}{\gamma-1}} \\ \overline{m}_{25} = k_4 \frac{P_{0,3}}{P_{0,25}} \sqrt{\frac{T_{0,25}}{T_{0,4}}} \end{cases} \tag{7}$$

The notation in equation (7) is standard with the numbered subscripts corresponding to states at entry to/exit from the components shown schematically in Figure 7.

An iterative process is required since both pressure ratios and non-dimensional mass-flows are dependent on the compressors' isentropic efficiencies, which, in turn, are functions of pressure ratios and non-dimensional mass-flows. The operating point thus depends (for a given system) only on the ratio $\frac{T_{0,4}}{T_{0,2}}$ (a function of the fuel flow or engine throttle), which can be regarded as the control variable of the system. It is clear how the

working-line becomes flatter for larger design pressure ratio compressors, leading to significant part-speed problems for large multi-stage compressors, generally attenuated through the use of variable guide vanes and/or bleed.[3] The IPC encounters a larger variation in operating point and its off-design performance must therefore be considered with particular care.

### *III.A.2. Off-design Operational Limits*

The design-point value for the ratio $\frac{T_{0,4}}{T_{0,2}}$ can be determined from the design-point performance, while excursions from this value depend on the engine and compressor operational limits. The design point is generally much closer to the maximum $\frac{T_{0,4}}{T_{0,2}}$, established by the maximum allowable turbine entry temperature and compressor rotational speed, than to its minimum, which then represents the most dangerous condition from an aerodynamic point of view.[4] The minimum value is normally encountered during engine idling operations (during descent) and can be calculated based on the blow out air-fuel ratio (a typical value for aircraft engine fuels is 250[17]). The temperature change in the combustion process can be calculated as a function of the air-fuel ratio and the fuel lower calorific value $H_v$ (43 MJ/kg is a typical value for aircraft fuels):

$$\Delta T_{comb} = \frac{\dot{m}_{fuel}}{\dot{m}} \frac{H_v}{c_p} \tag{8}$$

The minimum combustion temperature rise can be calculated from equation (8) and the minimum value for the ratio $\frac{T_{0,4}}{T_{0,2}}$ found by imposing the condition

$$\frac{T_{0,4}}{T_{0,2}} \geq \frac{T_{0,3} + \Delta T_{comb,min}}{T_{0,2}} = \left(\frac{T_{0,4}}{T_{0,2}}\right)_{min} = f(PR_{IPC}, PR_{HPC}, \eta_{IPC}, \eta_{HPC}) \tag{9}$$

## III.B. Uncertainty Propagation

A review of the main methods available for uncertainty propagation in physical systems was given in Section I, while an analysis of the system performance under off-design operating conditions was given in Section III.A.1, where the role of the ratio $\frac{T_{0,4}}{T_{0,2}}$ as the system's control variable was highlighted. As the compressor is expected to operate along its working-line for the majority of the time, only these conditions will be considered for the analysis and optimisation of robust performance. Safe transient operation must be ensured through a sufficient surge margin along the entire working-line. Several methods for calculating engine transients exist[5, 19] but will not be considered here because of the limited impact on mean performance.

Due to the large extent of the compressor working-line, methods based on the evaluation of the objective function derivatives (such as sensitivity analysis and moment methods) are unlikely to provide accurate results, while the computational cost of MCS is incompatible with the requirements of an optimisation process, unless used in conjunction with a surrogate model. For these reasons, interval analysis and Polynomial Chaos represent the most promising approaches for the problem at hand and will be analysed in more detail.

### *III.B.1. Interval Analysis*

When computational resources are limited or there is no detailed information on the distribution of the input uncertainties (or, in this case, on the power settings' PDF), interval analysis offers a simple way of evaluating the system's robustness, in the form of the maximum performance drop from its nominal value due to deviation from the design point. Compression systems require their off-design performance to be analysed in detail during the design process before any further decisions are made. This analysis is normally completed at the end of the preliminary design process. This approach, while guaranteeing that the minimum requirements are satisfied, introduces a further loop in the design process and, more importantly, does not ensure the design solution will be optimal with respect to this new requirement. The automation and integration of robustness analysis into the preliminary design process can lead simultaneously to improved design-point and off-design performance (or at least to a better understanding of the trade-offs between these two conflicting objectives) at the cost of an increase in computational time.

As mentioned, the proprietary code used for mean-line multi-stage compressor performance analysis can calculate off-design performance (as a function of non-dimensional rotational speed and mass-flow). The compressor working-line (Section III.A.1) is a function of design-point specifications, engine throttle and

efficiency variation. For a given value of $\frac{T_{0,4}}{T_{0,2}}$, an iterative procedure is needed to calculate the operating point and the relative efficiency. Given that the local search at the heart of the optimisation algorithm is based on a H&J move, the design under consideration does not change dramatically from one calculation to the next, and the iterative procedure converges in a limited number of steps (less than 5). The worst condition will be for the lowest value of $\frac{T_{0,4}}{T_{0,2}}$, as explained in Section III.A.2.

### III.C. Polynomial Chaos

If the PDF of the control variable $\frac{T_{0,4}}{T_{0,2}}$ is available, Polynomial Chaos offers a means of calculating high order information (mean, variance and successive moments) at a much reduced cost compared to MCS.

The roots of PC are to be found in the Homogeneous Chaos expansion first proposed by Wiener[27] who employed Hermite polynomials in terms of Gaussian random variables to express stochastic processes with finite variance. Cameron and Martin[1] demonstrated that "any Fourier-Hermite series of any functional $F(x)$ of $L_2(C)$ converges in the $L_2(C)$ sense to $F(x)$" (i.e. any variable with finite variance – or second order – can be represented exactly through a Homogeneous Chaos expansion). The natural application is modeling uncertainty propagation in physical applications: stochastic differential equations can be solved based on a truncated PC representation, employing Galerkin projections onto a finite subspace spanned by these polynomials as a way of simplifying the equations themselves.[6]

Any second order process $X(\theta)$ (where $\theta$ is a generic random event) can be represented in the form

$$X(\theta) = a_0 H_0 + \sum_{i_1=1}^{\infty} a_{i_1} H_1(\xi_{i_1}(\theta)) + \sum_{i_1=1}^{\infty} \sum_{i_2=1}^{i_1} a_{i_1 i_2} H_2(\xi_{i_1}(\theta), \xi_{i_2}(\theta)) + \\ + \sum_{i_1=1}^{\infty} \sum_{i_2=1}^{i_1} \sum_{i_3=1}^{i_2} a_{i_1 i_2, i_3} H_3(\xi_{i_1}(\theta), \xi_{i_2}(\theta), \xi_{i_3}(\theta)) + \cdots \tag{10}$$

where $H_n(\xi_{i_1}(\theta), ..., \xi_{i_n}(\theta))$ denotes the Hermite polynomial of order $n$ in terms of the multi-dimensional non-correlated standard Gaussian random variables $\boldsymbol{\xi} = (\xi_{i_1}, ..., \xi_{i_n})$ with zero means and unit variances. The general expression of Hermite polynomials is given by

$$H_n(\xi_{i_1}, ..., \xi_{i_n}) = e^{\frac{1}{2}|\boldsymbol{\xi}|^2} (-1)^n \frac{\partial^n}{\partial \xi_{i_1} \cdots \partial \xi_{i_n}} e^{-\frac{1}{2}|\boldsymbol{\xi}|^2} \tag{11}$$

For notational convenience, the Hermite Chaos (HC) expansion (equation (10)) can be rewritten as

$$X(\theta) = \sum_{j=0}^{\infty} \hat{a}_j \Psi_j(\boldsymbol{\xi}) \tag{12}$$

where there is a one-to-one correspondence between the functions $H_n(\xi_{i_1}, ..., \xi_{i_n})$ and $\Psi_j(\boldsymbol{\xi})$, and also between the coefficients $\hat{a}_j$ and $a_{i_1,...,i_n}$. The polynomial basis $\Psi_j(\boldsymbol{\xi})$ of HC forms a complete orthogonal basis, i.e.

$$\langle \Psi_i \Psi_j \rangle = \langle \Psi_i^2 \rangle \delta_{ij} \tag{13}$$

where $\delta_{ij}$ is the Kronecker delta and $\langle \cdot, \cdot \rangle$ denotes the ensemble average. This is the inner product in the Hilbert space of the Gaussian random variables

$$\langle f(\boldsymbol{\xi}) g(\boldsymbol{\xi}) \rangle = \int f(\boldsymbol{\xi}) g(\boldsymbol{\xi}) W(\boldsymbol{\xi}) d\boldsymbol{\xi} \tag{14}$$

where the weighting function $W(\boldsymbol{\xi})$ is

$$W(\boldsymbol{\xi}) = \frac{1}{(2\pi)^{n/2}} e^{-\frac{1}{2}|\boldsymbol{\xi}|^2} \tag{15}$$

The particularity that distinguishes the HC expansion from other types of expansion is the use of Hermite polynomials in terms of Gaussian random variables as the basis functions. Hermite polynomials are orthogonal with respect to the weighting function $W(\boldsymbol{\xi})$, which has the form of a multi-dimensional Gaussian PDF. The use of HC is particularly efficient when the input uncertainty is Gaussian-distributed (meaning

that it can be expressed through a first order HC expansion). Lucor *et al.*[18] demonstrated that an exponential convergence rate can be achieved in this case, while for differently distributed input uncertainties the convergence rate may be substantially slower.

### *III.C.1. Generalised Polynomial Chaos*

An extension of the HC expansion (named Wiener-Askey Polynomial Chaos) was proposed by Xiu and Karniadakis[28] to deal with more general random inputs more efficiently. The underlying concept remains the same (expansion of the generic random process through a set of orthogonal polynomials) but the Hermite polynomials basis is replaced by a generic basis of orthogonal polynomials. A random process $X(\theta)$ can still be expressed as

$$X(\theta) = c_0 I_0 + \sum_{i_1=1}^{\infty} c_{i_1} I_1(\xi_{i_1}(\theta)) + \sum_{i_1=1}^{\infty} \sum_{i_2=1}^{i_1} c_{i_1 i_2} I_2(\xi_{i_1}(\theta), \xi_{i_2}(\theta)) + \\ + \sum_{i_1=1}^{\infty} \sum_{i_2=1}^{i_1} \sum_{i_3=1}^{i_2} c_{i_1 i_2, i_3} I_3(\xi_{i_1}(\theta), \xi_{i_2}(\theta), \xi_{i_3}(\theta)) + \cdots \tag{16}$$

where $I_n(\xi_{i_1}(\theta), .., \xi_{i_n}(\theta)$ represents the Wiener-Askey polynomial of order $n$ in terms of the random vector $\boldsymbol{\xi} = (\xi_{i_1}, ..., \xi_{i_n})$. The polynomials $I_n$ now are not restricted to the Hermite polynomials but can be any orthogonal polynomials. For notational convenience, equation (16) can be rewritten as

$$X(\theta) = \sum_{j=0}^{\infty} \hat{c}_j \Phi_j(\boldsymbol{\xi}) \tag{17}$$

where there is a one-to-one correspondence between the polynomials $I_n(\xi_{i_1}, ..., \xi_{i_n})$ and $\Phi_j(\boldsymbol{\xi})$ and between the coefficients $\hat{c}_j$ and $c_{i_1,...,i_n}$. These polynomials are again orthogonal.

The PC basis and supporting distribution can be chosen from the Askey scheme (see Table 3) as most appropriate for the given input uncertainty distribution: this can allow (as in the case of Gaussian distributions and Hermite Chaos) certain input uncertainties to be expressed exactly through a first order expansion, simplifying significantly the task of solving the stochastic differential equations governing the problem and improving the accuracy of the solution. With this approach, Xiu and Karniadakis[28] achieved exponential convergence for a number of different input distributions.

Table 3: Orthogonal polynomials from the Askey scheme[28]

| | Random Variable | Polynomial Chaos Basis |
|---|---|---|
| Continuous | Gaussian | Hermite |
| | Gamma | Laguerre |
| | Beta | Jacobi |
| | Uniform | Legendre |
| Discrete | Poisson | Charlier |
| | Binomial | Krawtchouk |
| | Negative Binomial | Meixner |
| | Hypergeometric | Hahn |

### *III.C.2. Non-intrusive Polynomial Chaos*

Even though PC has been applied successfully to the solution of a wide range of problems, its application to the analysis of complex systems can be far from straightforward. Appropriate modification of the equations governing the system behaviour can be very time-consuming and the implementation of PC is non-trivial. Modern engineering design involves a large number of disciplines and quite often relies on third party software products, the modification of which to suit the needs of the PC approach is frequently out of the question. A non-intrusive alternative has been developed based on the observation that the coefficients of the different

modes can be obtained by projecting deterministic computations onto the PC basis:[15] considering Hermite Chaos

$$u_i = \frac{1}{\langle \Psi_i^2 \rangle} \int_{-\infty}^{+\infty} d\xi_1 \cdots \int_{-\infty}^{+\infty} d\xi_N u(\boldsymbol{\xi}) \Psi_i(\boldsymbol{\xi}) W(\boldsymbol{\xi}) \tag{18}$$

As $u(\boldsymbol{\xi})$ and $\Psi_i(\boldsymbol{\xi})$ are both polynomials ($\Psi_i$ is a polynomial by definition and the Cameron-Martin theorem ensures the convergence of the Fourier-Hermite representation of any functional with finite variance to the functional itself[1]), the above integral can be calculated exactly through a Gaussian quadrature formula

$$u_i = \frac{1}{\langle \Psi_i^2 \rangle} \sum_{n_1=1}^{N_0} \cdots \sum_{n_N=1}^{N_0} u(\xi_{n_1}, \cdots, \xi n_N) \Psi_i(\xi_{n_1}, \cdots, \xi n_N) \prod_{k=1}^{N} w_{n_k} \tag{19}$$

where the couples $(x_k, w_k)$ represent the one-dimensional Gaussian quadrature points and weights. This formula is exact when the integrand is a polynomial of degree less than or equal to $2N_0 - 1$.[20] The quadrature points are the zeros of the orthogonal polynomial of degree $N_0$ and the weights can be calculated as

$$w_k = \frac{1}{[\psi_n'(x_k)]^2} \int_{-\infty}^{+\infty} W(x) \left[ \frac{\psi_n(x)}{x - x_k} \right]^2 dx \tag{20}$$

in which $\psi_n'(x_k)$ is the first order derivative of the orthogonal polynomial of order $n$ at quadrature point $x_k$.

It is important to note that the number of deterministic calculations required by the non-intrusive PC (NIPC) approach is equal to $(N_0 + 1)^N$, which is always greater than the $\frac{(N_0+N)!}{N_0!N!}$ calculations required by intrusive PC[15] ($N$ is the number of random dimensions and $N_0$ the quadrature order). Nevertheless, the possibility of treating the analysis software as a black box is a significant advantage.

### *III.C.3. Non-standard Distributions*

As noted in Section III.C, the Cameron-Martin theorem[1] ensures the possibility of using HC to represent any second order process. In principle, any set of orthogonal polynomials from the Askey scheme (Table 3) can be used to express any distribution. Choosing the weighting function to match the random variable's input distribution (and choosing the PC basis as a consequence) has the advantage that the input random variable can be expressed exactly as a first order expansion with respect to the PC basis, simplifying significantly the computations and, more importantly, ensuring an exponential convergence. In the case of a non-standard distribution (or if, for any reason, a particular set of orthogonal polynomials is preferred) the input variable needs to be expressed as a function of the support variable (or, equivalently, the coefficients of its expansion in terms of the elements of the PC basis need to be determined). As for NIPC, the coefficients can be obtained by a projection of the generic input variable $k$ onto the PC basis:

$$k_i = \frac{\langle k \Phi_i \rangle}{\langle \Phi_i^2 \rangle} = \frac{1}{\langle \Phi_i^2 \rangle} \int_a^b k \Phi_i(\xi) W(\xi) d\xi \tag{21}$$

The main assumption here is that the variables $k$ and $\xi$ are fully correlated (i.e. a univocal relation exists between $\xi$ and $k$).[28] In this form, the integral in equation (21) cannot be evaluated as the variables $k$ and $\xi$ belong to two different probability spaces. By taking a support variable $x$, uniformly distributed in the interval (0,1), it is possible to apply a variable transformation such as

$$dx = f(k)dk = dF(k) \qquad dx = g(\xi)d\xi = dG(\xi) \tag{22}$$

where $f(k)$ and $g(\xi)$ are the PDFs of $k$ and $\xi$ respectively and $F(k)$ and $G(\xi)$ their cumulative distribution functions. It follows that

$$x = \int_{-\infty}^{k} f(t)dt = F(k) \qquad x = \int_{-\infty}^{\xi} g(t)dt = G(\xi) \tag{23}$$

and

$$k = F^{-1}(x) = h(x) \qquad \xi = G^{-1}(x) = l(x) \tag{24}$$

Equation (21) thus becomes

$$k_i = \frac{1}{\langle \Phi_i^2 \rangle} \int_a^b k \Phi_i(\xi) W(\xi) d\xi = \frac{1}{\langle \Phi_i^2 \rangle} \int_0^1 h(x) \Phi_i(l(x)) dx \tag{25}$$

The inverses of the cumulative distribution functions for some common distributions are known.[28] Alternatively, they can be calculated numerically given the corresponding PDFs.

### *III.C.4. Constructing Generic Orthogonal Polynomials*

A more efficient approach for handling non-standard distributions is to determine the set of orthogonal polynomials with respect to the generic distribution (which here has been normalised between 0 and 1 for simplicity). A generic expression for an orthogonal polynomial of order $m$ is

$$P_m(\xi) = \sum_{j=0}^{m} b_{m,j} \xi^j \tag{26}$$

The orthogonality condition can be expressed as

$$\int_0^1 P_m(\xi) W(\xi) \xi^k d\xi = 0 \qquad \text{for } k = 0, ..., m-1 \tag{27}$$

The integral in equation (27) simplifies significantly if the weighting function $W(\xi)$ can be expressed as a polynomial (or can be calculated numerically for a non-polynomial PDF)

$$W(\xi) = \sum_{i=0}^{n} a_i \xi^i \tag{28}$$

In this case

$$\int_0^1 P_m(\xi) W(\xi) \xi^k d\xi = \int_0^1 \sum_{j=0}^{m} b_{m,j} \xi^j \sum_{i=0}^{n} a_i \xi^i \xi^k d\xi = 0 \qquad \text{for } k = 0, ..., m-1 \tag{29}$$

The integrals in equation (29) give the following conditions:

$$\sum_{j=0}^{m} b_{m,j} \sum_{i=0}^{n} \frac{a_i}{i+j+k+1} = 0 \qquad \text{for } k = 0, ..., m-1 \tag{30}$$

The system in (30) has $m$ equations for $m+1$ unknowns (the coefficients of $P_m$). The remaining condition can come from the choice of a value for the intercept ($b_{m,0} = 1$ for example). This system of equations can then readily be solved, as detailed in.[7]

Application Consider the following non-standard multi-modal PDF, illustrated in Figure 8:

$$f(x) = 18.2342x - 95.2432x^2 + 164.5764x^3 - 87.5675x^4 \tag{31}$$

The basis of orthogonal polynomials with respect to this PDF can be determined as described above. The resulting orthonormal polynomials are reported in Table 4.

A first order expansion in terms of this new set of orthonormal polynomials (with respect to a weighting function with the same distribution as $f(x)$) will express the input distribution exactly. The roots of the generic orthonormal polynomial of degree $G$, the values of the orthonormal polynomials of degree less than $G$ at the quadrature points and the weights can now all be calculated.[7] The results are reported in Figure 9, where the order of the polynomial can be identified by recalling that a polynomial of degree $m$ has $m-1$ stationary points, and in Table 5.

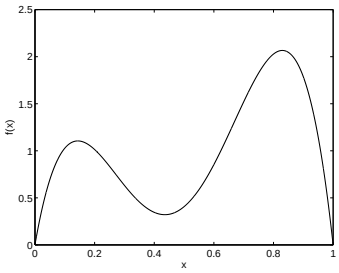


Figure 8: A non-standard probability density function

Table 4: System of orthonormal polynomials

| Order | $P_i^*$ | $\langle (P_i^*)^2 \rangle$ |
|---|---|---|
| 0 | $1$ | 1 |
| 1 | $2.0293 - 3.4512\xi$ | 1 |
| 2 | $2.6955 - 16.3218\xi + 16.0617\xi^2$ | 1 |
| 3 | $4.0995 - 42.7907\xi + 98.4216\xi^2 - 62.8152\xi^3$ | 1 |
| 4 | $5.0015 - 81.4621\xi + 347.0134\xi^2 - 524.4300\xi^3 + 258.0990\xi^4$ | 1 |
| 5 | $6.5207 - 149.9490\xi + 963.9440\xi^2 - 2444.9253\xi^3 + 2661.0726\xi^4 - 1041.7694\xi^5$ | 1 |
| 6 | $7.7384 - 237.3649\xi + 2133.9160\xi^2 - 8103.0401\xi^3 + 14720.2905\xi^4 ...$ $... - 12687.9273\xi^5 + 4172.7058\xi^6$ | 1 |

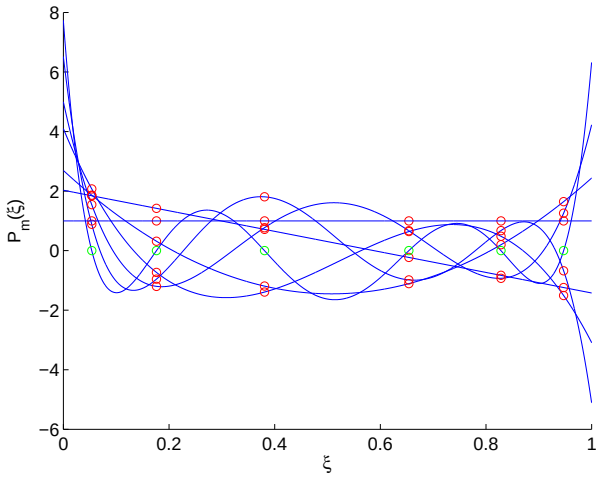


Figure 9: Orthonormal polynomials up to degree 6, with quadrature points values

Table 5: Roots and weights of a sixth order quadrature

| ROOT $\xi_i$ | WEIGHT $w_i$ | $P_0$ | $P_1$ | $P_2$ | $P_3$ | $P_4$ | $P_5$ |
|---|---|---|---|---|---|---|---|
| 0.0538 | 0.0652 | 1.0000 | 1.8436 | 1.8638 | 2.0723 | 1.5435 | 0.8841 |
| 0.1763 | 0.1665 | 1.0000 | 1.4208 | 0.3170 | -0.7299 | -1.1989 | -0.9582 |
| 0.3808 | 0.1146 | 1.0000 | 0.7150 | -1.1908 | -1.3917 | 0.7695 | 1.8071 |
| 0.6542 | 0.2437 | 1.0000 | -0.2284 | -1.1083 | 0.6407 | 0.6665 | -0.9837 |
| 0.8285 | 0.3053 | 1.0000 | -0.8299 | 0.1974 | 0.4829 | -0.9285 | 0.6723 |
| 0.9471 | 0.1046 | 1.0000 | -1.2394 | 1.6445 | -1.5083 | 1.2597 | -0.6773 |

The NIPC approach was applied to the system (IPC, duct and HPC) to evaluate the performance PDF for an input parameter $\frac{T_{0,4}}{T_{0,2}}$ with a PDF as in Figure 8. The results are compared with Monte Carlo Simulations in Figure 10: the convergence of the MCS results towards those given by NIPC is evident and the two curves

are almost indistinguishable for $10^5$ MCS. On the other hand, the difference in computational time required is striking: 6 simulations are sufficient for NIPC while some thousands are required for MCS.

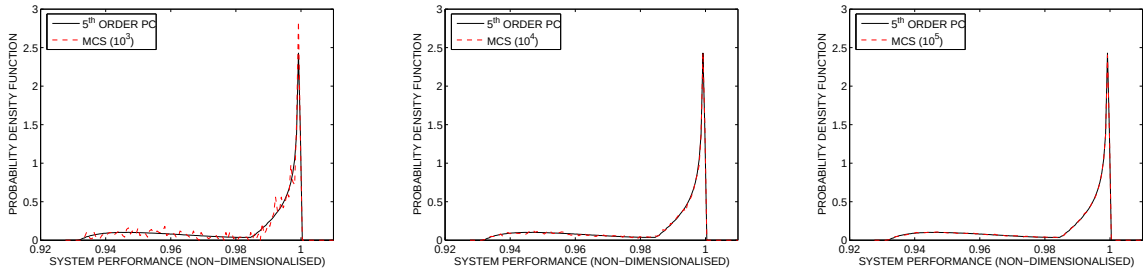


Figure 10: Convergence of Monte Carlo Simulations towards Polynomial Chaos

The relevant statistics can then be calculated. Only mean, variance and third order moment are reported (equations (32) *et seq.*):

$$\mu = \int_0^1 \sum_{i=0}^{p} y_i P_i(\xi) W(\xi) d\xi = y_0 \tag{32}$$

$$\sigma^2 = \int_0^1 \left( \sum_{i=0}^{p} y_i P_i(\xi) \right)^2 W(\xi) d\xi = \sum_{i=1}^{p} y_i^2 \tag{33}$$

$$s^3 = \int_0^1 \left( \sum_{i=1}^{p} y_i P_i(\xi) \right)^3 W(\xi) d\xi = \sum_{i=1}^{p} \sum_{j=1}^{p} \sum_{k=1}^{p} y_i y_j y_k \langle \Psi_i \Psi_j \Psi_k \rangle \tag{34}$$

where $y(\xi) = \sum_{i=0}^{p} y_i \Psi_i(\xi)$ is the response of the system in terms of the adopted PC expansion and the triple product $\langle \Psi_i \Psi_j \Psi_k \rangle$ can be calculated as

$$\langle P_i P_j P_k \rangle = \sum_{i_1=0}^{i} \sum_{i_2=0}^{j} \sum_{i_3=0}^{k} \sum_{i_4=0}^{n} \frac{b_{i,i_1} b_{j,i_2} b_{k,i_3} a_{i_4}}{i_1 + i_2 + i_3 + i_4 + 1} \tag{35}$$

where $n$ is the degree of the weighting function $W(\xi)$ (equation (28)).

# IV. Results

## IV.A. Interval Analysis

### *IV.A.1. A Posteriori Analysis*

An analysis of the off-design behaviour of the optimal designs obtained from the design-point optimisation completed in Section II is useful not only to verify the robustness of these solutions but also to gain a better understanding of their weaknesses. Figure 11 compares the design-point and part-load (for the limiting value of $\frac{T_{0,4}}{T_{0,2}}$) efficiencies of the maximum efficiency solutions, for both the 8-stage and 7-stage IPC configurations, together with the datum design. The 6-stage configuration is not included as the working-line crosses the surge-line before reaching the limiting value of $\frac{T_{0,4}}{T_{0,2}}$. All values are expressed as percentage changes from the design-point efficiency of the datum design. It is evident how the significant improvement in design-point performance is achieved at the price of a consistent deterioration in part-load efficiency.

### *IV.A.2. Robust Optimisation*

The aim of this optimisation problem is to maximise simultaneously design-point and off-design performance of the core compression system introduced in Section II. As shown, both part-load efficiency and operating margins are important objectives in compression system design: to avoid an excessive rise in computational costs, the operating margins have been considered here as inequality constraints, treated with penalty

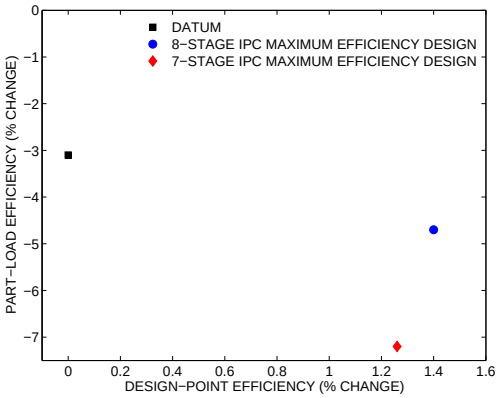


Figure 11: Design-point and limit performance for the maximum efficiency designs (all values relative to the design-point performance of the datum design)

functions to minimise the complexity of the design space. The optimisation problem (95 variables and 2 objectives) is summarised in Table 6.

Table 6: Definition of the first robust optimisation problem

| | |
|---|---|
| maximise | $f_1 = \eta_{is,dp} - a_1 \max\left[0, (\overline{SM}_{dp} - SM_{dp})\right]$ |
| | $f_2 = \eta_{is,pl} - a_2 \max\left[0, (\overline{SM}_{pl} - SM_{pl})\right]$ |
| subject to | $DH_{min} \geq \overline{DH}$ |
| | $SPR_{max} \leq \overline{SPR}$ |
| | $DF_{max} \leq \overline{DF}$ |
| | $Koch_{max} \leq \overline{Koch}$ |
| | $H_{max_{DUCT}} \leq \overline{H}$ |

The optimisation run took approximately 3 days on an AMD Athlon 2.0 GHz machine, for a total of 1,200 optimisation steps and 48,000 solutions evaluated.

The results from this robust optimisation are reported in Figure 12: it is evident than substantial improvements in off-design performance can be achieved without compromising excessively the design-point efficiency, for both the 8-stage and 7-stage IPC configurations. Figure 12(b) shows the variation of the design variables' values for the non-dominated solutions (8-stage IPC). It is evident that only the first 55 design variables (defining the IPC and duct designs) exhibit appreciable variations, while the remaining variables are almost fixed at their initial values (the non-robust solution), reflecting the larger operating range of the IPC, the off-design performance of which needs to be considered with particular care.

## IV.B. Polynomial Chaos

### *IV.B.1. A Posteriori Analysis*

As for the interval analysis approach, the optimal designs obtained from the non-robust optimisation of Section II have been analysed using the PC approach to verify their mean performance. The PDF of Figure 8 has been assumed for the ratio $\frac{T_{0,4}}{T_{0,2}}$, with one maximum near the design point and one for a lower value, near idling. A different PDF (more closely reflecting real engine usage) could be substituted if available, without requiring any modifications to the method developed here; the general conclusions of this section would remain still valid. Figure 13 shows the results from the robust analysis of the core compression system configurations that are optimal with respect to design-point performance, expressed as a function of IPC and HPC surge margins and mean system isentropic efficiency. The conclusion is the same as that already reached with the interval analysis approach (Section IV.A.1): the improvements in mean efficiency are substantially lower than those in design-point efficiency, because of the worse off-design behaviour of the improved design-point efficiency solutions.

Figure 14 reports only the non-dominated designs. Only 15% of the original Pareto front is non-dominated, suggesting that better designs (from an overall performance point of view) can probably be

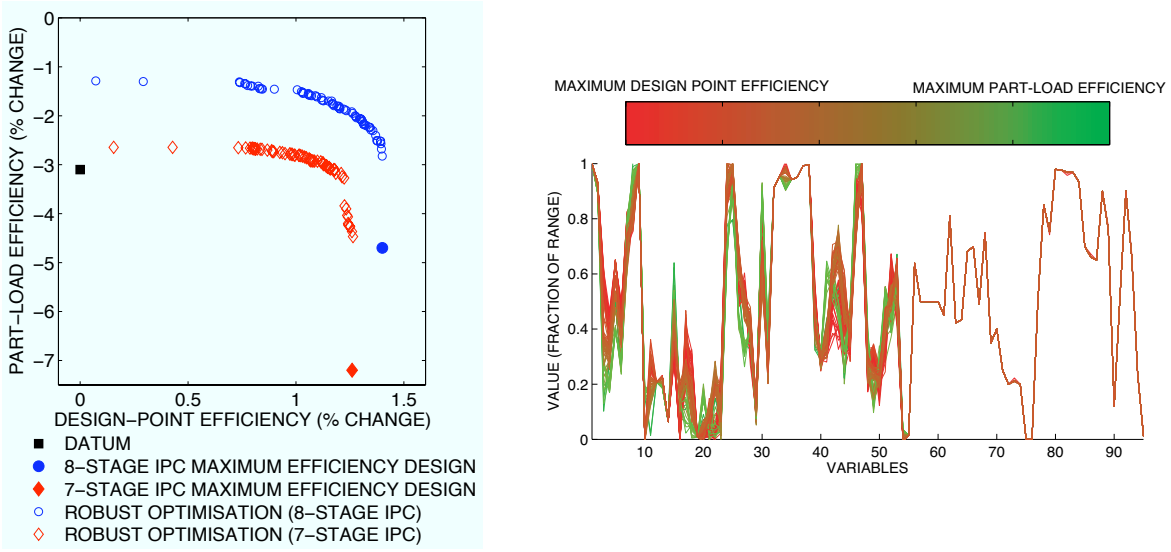


(a) Pareto fronts

(b) Design variables (as parallel coordinates)

Figure 12: Results for the first robust optimisation problem

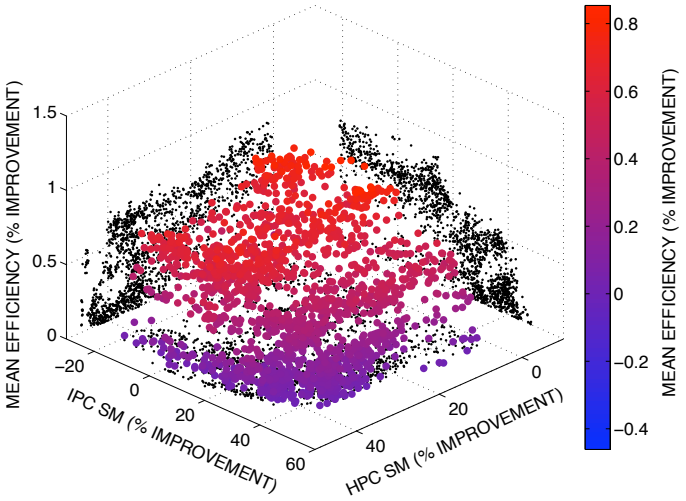


Figure 13: Robust analysis of the optimal designs of Section II

obtained by integrating robustness analysis in the optimisation process.

In Figure 15 the maximum values of design-point and mean efficiency are compared as a function of IPC and HPC surge margins. The drop in mean performance is due to the sub-optimal off-design behaviour of the design solutions resulting from the optimisation of the design-point performance alone.

### *IV.B.2. Robust Optimisation*

The optimisation problem is similar to that of Section II. The mean efficiency has replaced the design-point value as an objective, while a minimum part-speed surge margin has been guaranteed through a penalty function. The variance of the system efficiency from its mean value has been not considered in the optimisation problem so as not to increase the computational costs even further, and because of the greater importance of the mean value from a design point of view (the mean value of the efficiency – not its variance – has a direct impact on the mean cycle efficiency). Furthermore, having verified that design-point efficiency and part-load efficiency are competing objectives, maximisation of mean performance will naturally lead to a

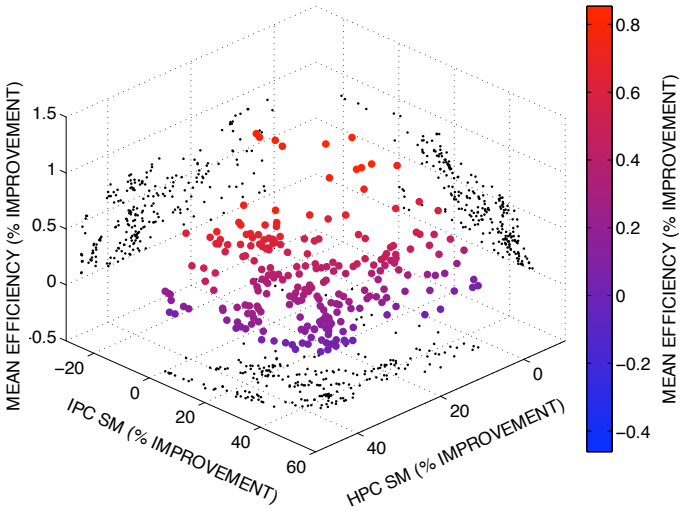


Figure 14: Non-dominated robust designs from the optimal designs of Section II

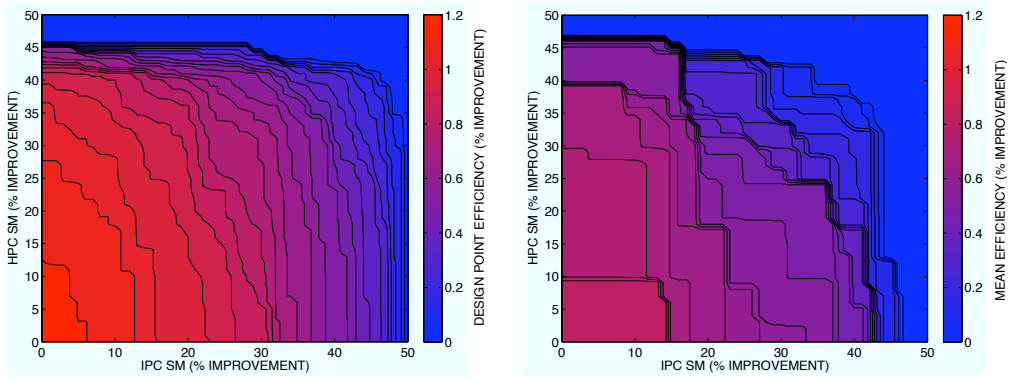


(a) Design-point efficiency

(b) Mean efficiency

Figure 15: Comparison of design-point and mean efficiency for the optimal designs from Section II

minimisation of its variance. Safe off-design behaviour is, in any case, guaranteed through the use of penalty functions. The optimisation problem is summarised in Table 7. The total run-time was about 3 weeks on an AMD Athlon 2.0 GHz machine, for 3,500 optimisation steps and about 140,000 solution evaluations.

Table 7: Definition of the second robust optimisation problem

| | |
|---|---|
| maximise | $\mu_\eta$ |
| | $SM_{IPC}$ |
| | $SM_{HPC}$ |
| subject to | $DH_{min} \geq \overline{DH}$ |
| | $SPR_{max} \leq \overline{SPR}$ |
| | $DF_{max} \leq \overline{DF}$ |
| | $Koch_{max} \leq \overline{Koch}$ |
| | $H_{max_{DUCT}} \leq \overline{H}$ |

The results are reported in Figure 16: again, a consistent improvement in performance can be achieved through the robust optimisation approach. A fundamental difference between this and the optimisation of Section II is the sparsity of points in the low IPC surge margin region of the Pareto front, due to the flatness of this region, and thus to the minimal improvements in mean efficiency that are possible for lower values of the IPC surge margin. This result is consistent with the large extent of the IPC working-line, and thus

with the better off-design performance achievable from a compressor with a larger design-point surge margin. The same is even more evident in Figure 17, where the maximum value of efficiency achievable for a given combination of IPC and HPC surge margins is reported.

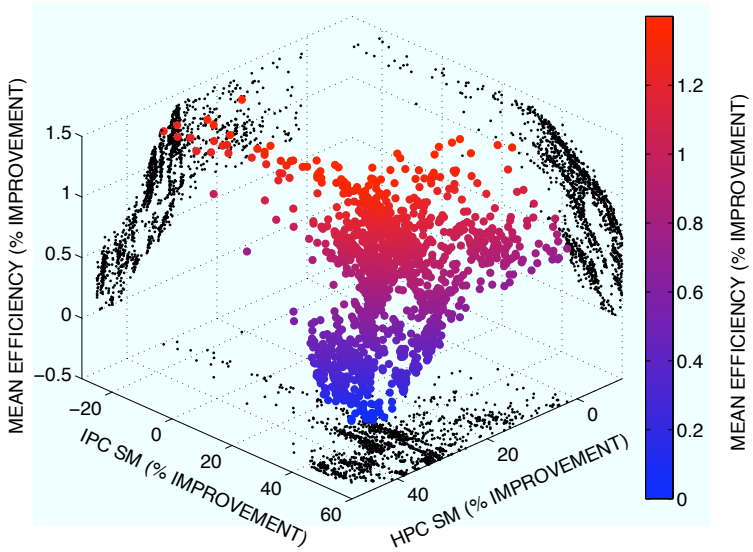


Figure 16: Pareto front for the robust optimisation using Polynomial Chaos

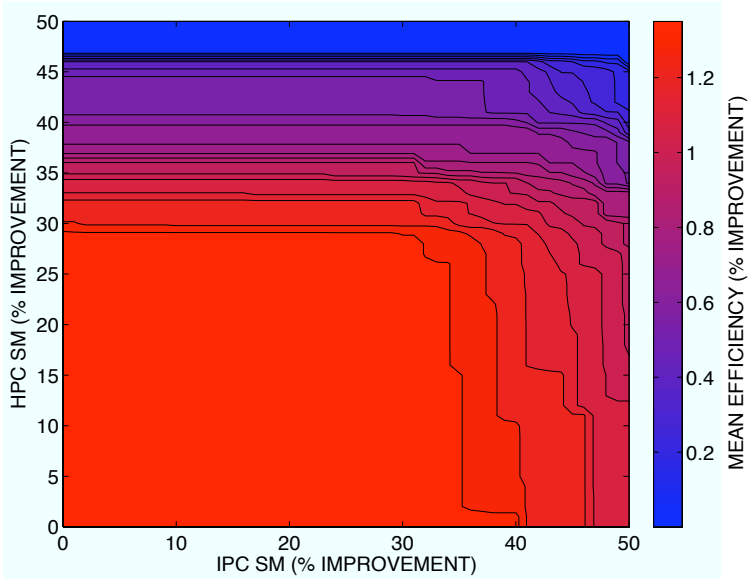


Figure 17: Efficiency contours for the robust optimisation using Polynomial Chaos

## V. Conclusions

Complexity in gas turbine design has traditionally been managed through a modular approach, where a conceptual design phase fixes the values for some global parameters and dimensions in order to subdivide the overall task into simpler problems. Apart from the subdivisions present between different modules, further fragmentation is present within the design of each module, both relative to the level of fidelity and among disciplines. Jarrett *et al.*[13] and Ghisu *et al.*[9] demonstrated how significant improvements can be achieved through a reduction in the level of fragmentation and modularity of the current design process, while a consistent reduction in development time is possible through the elimination of a number of iteration loops

required by the modular approach before all the constraints are satisfied simultaneously. In the resulting large and complex design space – with several objectives and constraints to be considered concurrently – the chances of being able to locate the optimal design by simple trial-and-error (or "design-by-analysis") are next to nil: a more intelligent search approach – design optimisation – is essential to achieve a satisfactory exploration of the design space, leading to improved designs and a reduction in the development time thanks to the automation of the whole process.

A common simplification in the design of gas turbine engines is to consider nominal operating conditions (the design point) during the design process, while off-design operation is considered only at a later stage. While guaranteeing that some minimum requirements are met, this approach introduces a further loop into the design process and, more importantly, is very unlikely to lead to a product with optimal design-point and off-design performance. If design-point performance is considered as the only objective in the optimisation, the risk is that the off-design behaviour will be (significantly) worse (a common situation for heavily optimised products[14]). In this case, is the optimised design really better than the original one? Only the inclusion of a figure of merit quantifying robustness in the optimisation problem can produce a design with better design-point and off-design behaviour or, at least, provide a trade-off between the two performance metrics.

As the aim of this work is to incorporate robustness analysis in the optimisation process, the computational cost of each robustness evaluation is of fundamenteal importance: two methods – one deterministic (interval analysis) and one stochastic (Polynomial Chaos) – are presented and integrated into a representative design system. Both methods are able to identify solutions that are significantly more robust (or less sensitive to changes in operating conditions) than those found by the traditional optimisation approach.

## References


[1]R. H. Cameron and W. T. Martin. The orthogonal development of non-linear functionals in series of Fourier-Hermite polynomials. *Annals of Mathematics*, 48(2):385–392, 1947.

[2]H. Choen, G. F. C. Rogers, and H. I. H. Saravanamuttoo. *Gas Turbine Theory*. Longman Scientific & Technical, UK, 1987.

[3]N. A. Cumpsty. *Compressor Aerodynamics*. Longman Scientific & Technical, UK, 1989.

[4]N. A. Cumpsty. *Jet Propulsion*. Cambridge University Press, UK, 1997.

[5]R. D. Flack. *Fundamentals of Jet Propulsion with Applications*. Cambridge University Press, UK, 2005.

[6]R. Ghanem and P. Spanos. *Stochastic Finite Elements: A Spectral Approach*. Springer-Verlag, New York, 1991.

[7]T. Ghisu. *Robust Aerodynamic Design of Compression Systems*. PhD thesis, University of Cambridge, Cambridge, UK, 2008.

[8]T. Ghisu, M. Molinari, G. T. Parks, W. N. Dawes, J. P. Jarrett, and P. J. Clarkson. Axial compressor intermediate duct design and optimisation. In *3rd AIAA Multidisciplinary Design Optimization Specialist Conference*, Honolulu, Hawaii, USA, 2007.

[9]T. Ghisu, G. T. Parks, J. P. Jarrett, and P. J. Clarkson. Integrated design optimisation of gas turbine compression systems. In *4th AIAA Multidisciplinary Design Optimization Specialist Conference*, Chicago, Illinois, USA, 2008.

[10]F. Glover and M. Laguna. *Tabu Search*. Kluver Academic Publisher, USA, 1997.

[11]R. Hooke and T. A. Jeeves. 'Direct search' solution of numerical and statistical problems. *Journal of the Association for Computing Machinery*, 2(8):212–229, 1961.

[12]D. M. Jaeggi, G. T. Parks, T. Kipouros, and P. J. Clarkson. The development of a multi-objective Tabu Search algorithm for continuous optimisation problems. *European Journal of Operational Research*, 185:1192–1212, 2008.

[13]J. P. Jarrett, T. Ghisu, and G. T. Parks. On the coupling of designer experience and modularity in the aerothermal design of turbomachinery. In *ASME Paper GT2008-50131*, 2008.

[14]A. J. Keane and P. B. Nair. *Computational Approaches for Aerospace Design*. Wiley, 2005.

[15]O. P. Le Maître, M. P. Reagan, H. N. Najm, R. G. Ghanem, and O. M. Knio. A stochastic projection method for fluid flow: part i, basic formulation. *Journal of Computational Physics*, 173(2):481–511, 2001.

[16]O. P. Le Maître, M. P. Reagan, H. N. Najm, R. G. Ghanem, and O. M. Knio. A stochastic projection method for fluid flow: part ii, random process. *Journal of Computational Physics*, 181(1):9–44, 2002.

[17]A. H. Lefebvre. *Gas Turbine Combustion*. Taylor & Francis, Philadelphia, USA, 1998.

[18]D. Lucor, D. Xiu, and G. Karniadakis. Spectral representations of uncertainty in simulations: algorithms and applications. *Journal of Fluids Engineering*, 124:51–59, 2002.

[19]J. D. Mattingly. *Elements of Gas Turbine Propulsion*. McGraw-Hill, USA, 1996.

[20]G. Monegato. *Fondamenti di Calcolo Numerico*. Edizioni Clut, Torino, Italy, 1998.

[21]W. L. Oberkampf and T. G. Trucano. Verification and validation in Computational Fluid Dynamics. *Progress in Aerospace Sciences*, 38:209–272, 2002.

[22]M. S. Phadke. *Quality Engineering using Robust Design*. Prentice-Hall International Editions, USA, 1989.

[23]M. M. Putko, P. A. Newman, A. C. Taylor, and L. L. Green. Approach for uncertainty propagation and robust design in CFD using sensitivity derivatives. In *AIAA 2001-2528*, 2001.

[24]P. J. Ross. *Taguchi Techniques for Quality Engineering*. McGraw-Hill, USA, 1996.

[25]P. P. Walsh and P. Fletcher. *Gas Turbine Theory*. Blackwell Science Ltd, UK, 1998.

[26]R. W. Walters and L. Huyse. Uncertainty analysis for fluid mechanics with applications. CR 0211449, NASA, 2002.

[27]N. Wiener. The homogeneous chaos. *American Journal of Mathematics*, 60(4):897–936, 1938.

[28]D. Xiu and G. E. Karniadakis. The Wiener–Askey polynomial chaos for stochastic differential equations. *SIAM Society for Industrial and Applied Mathematics*, 24(2):619–644, 2002.

[29]D. Xiu, D. Lucor, C.-H. Su, and G. E. Karniadakis. Stochastic modeling of flow-structure interaction using generalized pynomial chaos. In *ICOSAHOM-01*, Uppsala (SW), 2002.

[30]C. Zang, M. I. Friswell, and J. E. Mottershead. Probabilistic approach to free-form airfoil shape optimization under uncertainty. *Computers and Structures*, 83:315–326, 2005.